(54) Ahn, D. J.; Franses, E. I. *J. Chem. Phys.* **1991**, *95*, 8486.
(55) Wahlgren, M.; Arnebrant, T. *J. Colloid Interface Sci.* **1990**, *136*, 259.
(56) Evans, S. D.; Sharma, R.; Ulman, A. *Langmuir* **1991**, *7*, 156.
(57) Snyder, R. G. *J. Mol. Spectrosc.* **1960**, *4*, 411.
(58) Allara, D. L.; Nuzzo, R. G. *Langmuir* **1985**, *1*, 45.
(59) Outka, D. A.; Stöhr, J.; Rabe, J. P.; Swalen, J. D.; Rotermund, H. H. *Phys. Rev. Lett.* **1987**, *59*, 1321.
(60) Rabe, J. P.; Swalen, J. D.; Outka, D. A.; Stöhr, J. *Thin Solid Films* **1988**, *159*, 275.
(61) In ref 59, the average tilt angle of the chain axes of cadmium arachidate monomolecular film was reported to be less than 15° as measured by NEXAFS. The reason for the difference between their result and the present one is unclear at present. Possible reasons may be the following: (i) difference in surface roughness of the solid substrates used; (ii) different experimental conditions, for example, use of buffer solution; or (iii) different techniques (NEXAFS vs FTIR–ATR).
(62) Naselli, C.; Rabolt, J. F.; Swalen, J. D. *J. Chem. Phys.* **1985**, *82*, 2136.
(63) Naselli, C.; Rabe, J. P.; Rabolt, J. F.; Swalen, J. D. *Thin Solid Films* **1985**, *134*, 173.
(64) Cohen, S. R.; Naaman, R.; Sagiv, J. *J. Phys. Chem.* **1986**, *90*, 3054.
(65) Rabe, J. P.; Novotny, V.; Swalen, J. D.; Rabolt, J. F. *Thin Solid Films* **1988**, *159*, 359.
(66) Scherer, J. R.; Snyder, R. G. *J. Chem. Phys.* **1980**, *72*, 5798.
(67) Senak, L.; Moore, D.; Mendelsohn, R. *J. Phys. Chem.* **1992**, *96*, 2749.
(68) If one uses $n_2 = 1.55$ instead of 1.5, the average tilt angles of chain axes and transition moments are ca. 3° higher and 2° lower, respectively, for the systems studied.

The Inhibiting Effects of Tetraalkylammonium Cations on Simple Heterogeneous Electron Transfer Reactions in Polar Aprotic Solvents

W. Ronald Fawcett,* Milan Fedurco, and Marcin Opallo

Department of Chemistry, University of California, Davis, California 95616 (Received: June 26, 1992; In Final Form: August 28, 1992)

Kinetic data for the electroreduction of nitromesitylene at mercury in propylene carbonate have been determined in the presence of tetraalkylammonium salts of varying chain length, both as a function of electrode potential and temperature. Although the standard rate constant decreases with increase in cation size, the experimental activation enthalpy is independent of the cation for variation in this ion from tetraethylammonium to tetraoctylammonium. These results indicate that the tetraalkylammonium ions are adsorbed on the electrode forming a blocking layer whose thickness increases with alkyl chain length. Electron transfer to the redox center takes place by tunneling through this film. Theoretical estimates of the activation enthalpy support this conclusion and suggest that the redox reaction occurs in a region where solvent reorganization determines the largest portion of its magnitude.

Introduction

Studies of electrode kinetics are almost always carried out in the presence of an inert electrolyte in order to keep solution conductivity reasonably high and prevent migration as a means of mass transfer. In nonaqueous media, the salts used for this purpose often involve tetraalkylammonium cations (TAA⁺) because of their good solubility and weak tendency to form ion associates with anions in the system. However, it has been found in a number of studies[1–7] that the kinetics of simple electron transfer reactions involving organic molecules depend on the nature of the TAA⁺ ion, the usual trend being that the rate constant decreases with increase in the size of the alkyl group.[1–7] An interesting exception occurs when the TAA⁺ cation is not symmetrical with respect to the alkyl groups.[2]

On the basis of this work, a general picture of the effect of TAA⁺ ions on the kinetics of simple electron transfer reactions is beginning to emerge. In general, it seems clear[1,3,7] that the magnitude and direction of the double layer effect resulting from the presence of these ions cannot be predicted by the Frumkin model according to which the location of the reaction site is coincident with the outer Helmholtz plane (oHp).[8] Petersen and Evans[6] showed that the inhibiting effect of the tetraheptylammonium (THpA⁺) cation with respect to that of the tetraethylammonium (TEA⁺) cation became more pronounced for reactions occurring at more negative potentials. This suggests that TAA⁺ ions adsorb more strongly at the electrode/solution interface at more negative potentials, and thus have a greater inhibitory effect. Another important source of experimental information is the activation enthalpy obtained from the temperature dependence of the standard rate constant. This quantity is often independent of the nature of the TAA⁺ cation within experimental error;[1,3,6] however, it does depend on cation nature when the orientation of the reactant in the double layer results in variation in the effect of the TAA⁺ cation on the transition state with variation in its size.[1] Petersen and Evans[6] suggested on the basis

of their results that the probability of electron transfer through a TAA⁺ cation monolayer at the interface decreases with increase in cation size.

The purpose of the present study was to extend previous work in a systematic way by obtaining kinetic data, especially, the activation enthalpy, for a simple reaction with a wide range of tetraalkylammonium electrolytes for which the number of carbon atoms in the alkyl group varies from two to eight. The reaction chosen is the electroreduction of nitromesitylene (NM) at a mercury electrode, a system which has been investigated under a wide variety of conditions.[4,9–11] The solvent chosen is propylene carbonate (PC) which has a high dielectric constant (64.9 at 25 °C[12]) so that ion pairing effects are expected to be relatively unimportant. Moreover, in this system the reaction occurs at fairly negative charge densities on the electrode where the double layer capacity does not change significantly with potential.[13] This is important when one wants to obtain precise data with the ac admittance technique used for the present study.

Experimental Section

Materials. Nitromesitylene (1-nitro-2,4,6-trimethylbenzene) (Aldrich) and cobalticinium hexafluorophosphate (Strem) were used as received. All salts, tetraethylammonium (TEAP), tetrapropylammonium (TPAP), tetrabutylammonium (TBAP), tetrahexylammonium (THxAP), and tetraoctylammonium (TOAP) perchlorates (Fluka), were twice recrystallized from a water–methanol mixture and dried under reduced pressure at 70 °C for 24 h. AgClO₄ (Strem) was used as received. The solvents, propylene carbonate (Burdick & Jackson) and acetonitrile (AN) (HPLC grade, Aldrich), were purified as previously described.[14,15] The nitrogen used for electrochemical experiments and distillations was 99.998% pure.

Apparatus. The apparatus for phase sensitive ac admittance voltammetry was similar to that described previously.[14,15] The Solartron 1250 frequency response analyzer served as a source

of dc potential and sinusoidal perturbation (10 mV peak-to-peak). This signal was fed into the external input of an EG&G/PAR 273 potentiostat through a low impedance, purely resistive attenuator (10:1). The output of the current follower and reference signal from the potentiostat were fed into two channels of the same analyzer to obtain the in- and out-of-phase components of admittance. The advantage of using a two channel analyzer is that the phase shift of the potentiostat can be easily overcome.[15,16] The phase shift connected with other elements of the circuit was corrected using a dummy cell consisting of a resistance and capacitance in a range appropriate to the real system. Data acquisition and drop time were controlled by a dedicated microcomputer through a DAS-16 interface board.

Measurements were performed in a three electrode cell similar to that previously described[16] under a nitrogen atmosphere. A fine tipped dropping mercury electrode with flow rate in the range 0.03–0.10 mg s^{-1} adjusted by nitrogen pressure was used as a working electrode. A Pt cylinder surrounding the capillary tip of the working electrode served as counter electrode. The reference electrode consisted of a Ag wire immersed in a solution of 0.01 M AgClO$_4$ and 0.09 M TAAP in AN separated from working solution by a ceramic tip (Bioanalytical Systems). The solution in reference electrode compartment was changed every day in order to maintain potential stability, the TAA$^+$ salt being the same as that in the main cell. All potentials are reported with respect to the standard potential of the cobaltacenium/cobaltacene (COB$^+$/COB) systems measured in each solution. The temperature of the cell was controlled to a precision of ±0.5 °C by circulating a constant temperature fluid in a jacket surrounding the cell using a Brinkmann circulator (RM 6).

Procedures. All measurements were performed with a reactant concentration of 1 mM and with 0.1 M TAAP as supporting electrolyte. The dc reversibility of the studied systems was eventually ascertained from the slope of a plot of dc potential against log $[(i_d - i)/i]$. From the same plot the half wave potential, $E_{1/2}$, was also found. Diffusion coefficients were determined from dc polarographic diffusion limited currents at a drop time of 5 s with correction for spherical diffusion.[16,17] The ac admittance was measured after 4.5 s of drop growth at seven frequencies in the 100–1500 Hz range at 4 mV intervals in a potential range of 0.3 V symmetrical with respect to $E_{1/2}$. After phase correction, a blank line correction for both the in- and out-of-phase components of admittance was carried out using the data for the first and last five points of this potential range.

The rate constants, k, were obtained from the ratio of the slope and intercept of a Randles plot using the procedure described by Andreu et al.[18] This method allows determination of the standard rate constant, k_s, without assuming a value for the transfer coefficient, α_{ex}. The latter parameter was estimated from the slope of a logarithmic plot of the rate constant against overpotential. The error involved in estimating k_s and α_{ex} did not exceed 10% and 0.1, respectively. The activation enthalpy (ΔH_{ex}) was estimated from plots of ln k_s against reciprocal temperature $1/T$, the associated error being in the range from 0–10%. The differential capacity of the mercury/solution interface in PC was obtained by analysis of admittance data measured in the absence of the reactant. The potentials of zero charge (E_{pzc}) were estimated from the charging current profile in the dc experiment. In order to monitor the possible influence of adsorption kinetics on both kinetic and double layer data, measurements were also made at a longer drop time, namely, 9.5 s in 0.1 M THxAP and TOAP. No significant difference between these results and those obtained at shorter drop times was observed.

Results and Discussion

Double Layer Studies. Values of the potential of zero charge (pzc), E_{pzc}, determined in 0.1 M TAAP solutions in PC at a dropping mercury electrode are recorded in Table I. This potential becomes significantly more positive as the length of the alkyl group increases, suggesting that the TAA$^+$ cation specifically adsorbs at Hg to an increasing extent with increase in cation size. A similar effect was noted recently in a study of the double layer
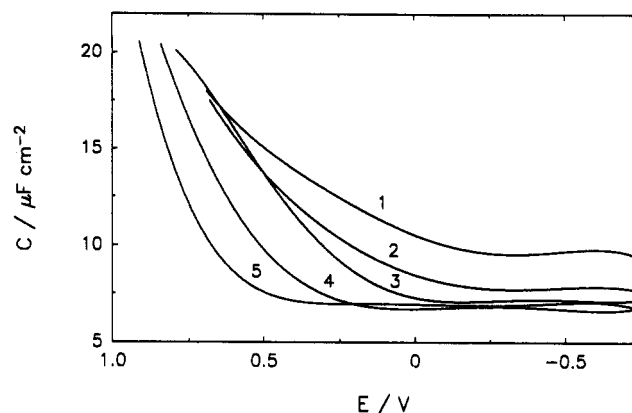

Figure 1. Differential capacity, C, of the mercury/propylene carbonate solution interface plotted against electrode potential, E, measured with respect to the standard potential for the cobaltacenium/cobaltacene reaction for 0.1 M solutions of various tetraalkylammonium perchlorates: (1) TEAP, (2) TPAP, (3) TBAP, (4) THxP, and (5) TOAP.
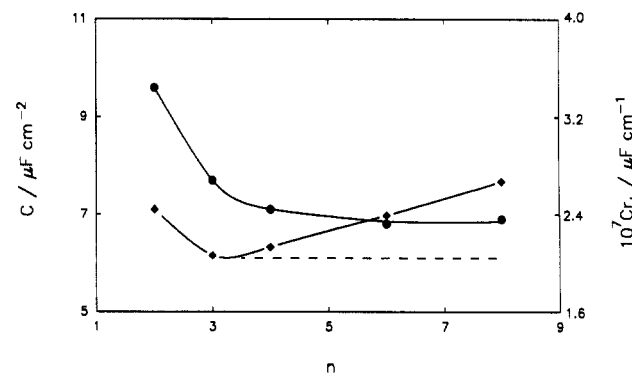

Figure 2. Differential capacity, C, measured at the standard potential for reduction of nitromesitylene (●) in solutions of various tetraalkylammonium perchlorates and the product of the differential capacity times the crystallographic radius of the electrolyte cation, Cr_+ (◆), plotted against the number of carbon atoms, n, in the alkyl chain of the cation. The left hand ordinate scale applies to the capacity data, and the right hand scale, to the Cr_+ data. The dashed line shows the limiting value of Cr_+ for the case that the alkyl chains are bent at the surface so that the charge center of the TAA$^+$ can approach closer to the electrode thereby making the effective cation radius smaller.

TABLE I: Electrolyte and Double Layer Parameters for 0.1 M TAAP Solutions at the Hg/PC Interface

electrolyte	cation crystallographic radius^a r_+, nm	potential of zero charge^b E_{pzc}	double layer capacity^c C, μF cm^{-2}
TEAP	0.337	0.678	9.6
TPAP	0.372	0.682	7.7
TBAP	0.413	0.788	7.1
THxAP	0.469	0.838	6.8
TOAP	0.503	0.906	6.9

^{a} From the compilation of Marcus.[19] ^{b} With respect to the standard potential for the cobaltacene/cobaltacenium cation couple in the given electrolyte. ^{c} At the standard potential for the nitromesitylene electroreduction in the given electrolyte.

capacity at the Hg/AN interface in the presence of TAA$^+$ ions of increasing size up to tetraheptylammonium (THpA$^+$).[20] Differential capacity data determined from the admittance data measured in the absence of the reactant at potentials negative of the pzc are shown in Figure 1. In all cases, the double layer capacity decreases as the potential becomes more negative becoming approximately constant in the most negative range. In addition, at the most negative potentials the capacity decreases with increase in cation size being approximately constant for the three largest cations studied. This trend is the same at the standard potential for electroreduction of NM (Table I and Figure 2). Similar trends were seen in earlier studies of the behavior of TAA$^+$
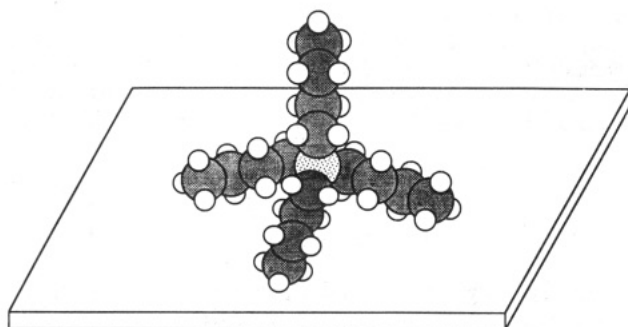
Figure 3. Diagram of a tetrabutylammonium ion on a surface with three of the tetrahedral arms in contact. As the attractive electrical field increases, the alkyl arms can bend to bring the central positive nitrogen atom closer to the surface.

cations in the double layer in PC,[13] AN,[20,21] and in dimethylformamide (DMF).[22] The capacity data also support the conclusion that the TAA^+ ions are contact adsorbed on Hg from PC solutions.

Two effects must be considered in understanding the variation in capacity with electrode potential and cation size. On one hand, as the potential becomes more negative, TAA^+ ions replace solvent molecules at the interface, and the dielectric constant of the inner part of the double layer decreases. Secondly, as the size of the cation increases for constant charge density on the electrode, the thickness of the inner layer should increase and the double layer capacity should decrease. On the basis of a simple parallel plate capacitor model, the inner layer capacity, C_i, is given by

$$C_i = \epsilon_i \epsilon_o / d_i \qquad (1)$$

where ϵ_i is the effective dielectric constant of the inner layer, ϵ_o, the permittivity of free space, and d_i, the thickness of the inner layer. In the present case where capacity data are examined at far negative potentials, the observed capacity C may be assumed to equal that of the inner layer C_i. If one also assumes that d_i is equal to the crystallographic radius of the TAA^+ ion, r_+ (see Table I), then the product $r_+ C$ should give an indication of the variation in the dielectric properties of the inner layer with cation size. Values of $r_+ C$ determined at the standard potential for NM reduction are also plotted as a function of the number of carbon atoms, n, in the alkyl group of the cation in Figure 2. It is apparent that $r_+ C$ reaches a minimum at $n = 3$ and then slowly rises as n increases. As the size of the TAA^+ cation increases, one would expect the inner layer dielectric constant to become constant at sufficiently negative potentials where the alkyl chains of these ions become the majority component of the inner layer. Then the product $r_+ C$ should be constant. One reason why this is not seen from the experimental results is that the assumed thickness of the inner layer may be somewhat less than the crystallographic radius of the TAA^+ ion. Since the alkyl chains are flexible to a certain extent, they may bend to allow the charge center of the cation to come closer to the surface (see Figure 3). In this case, the minimum value of $r_+ C$ should correspond to the limiting value of $\epsilon_i \epsilon_o$ and yield the effective thickness of the inner layer for larger TAA^+ cations at the most negative charge densities. From the present results this corresponds to 2.85×10^{-11} F m^{-1} giving an inner layer dielectric constant of 3.2 and a thickness of 0.37 nm. Accordingly, the smaller cations, TEA^+ and TPA^+, are not distorted when they are adsorbed, but the larger TBA^+, $THxA^+$, and TOA^+ ions have three alkyl chains on the surface bent so that the distance from the charge center of the ion to the surface is approximately 0.37 nm. A similar model for the structure of the Hg/AN interface in the presence of TAA^+ ions was proposed by Nielaba et al.[23] However, they concluded that the charge center of the N atom was much closer to the electrode, namely, 0.125 nm, effectively, the distance from the N atom to the surface when a tetramethylammonium cation (TMA^+) is located at the oHp. Such an assumption leads to a much smaller value for the effective dielectric constant, ϵ_i. It should also be noted that according to the present results, the value of ϵ_i for the TEA^+ system is larger

TABLE II: Thermodynamic and Kinetic Parameters for the Electroreduction of Nitromesitylene in Propylene Carbonate with Various 0.1 M TAAP Electrolytes

electrolyte	standard potential[a] E_s, V	standard rate constant k_s, cm s^{-1}	exptl transfer coeff[b] α_{ex}	exptl activation enthalpy[c] ΔH^*_{ex}, kJ mol^{-1}
TEAP	−0.427	0.289	0.53	26.0
TPAP	−0.434	0.167	0.52	28.3
TBAP	−0.427	0.087	0.50	30.2
THxAP	−0.440	0.041	0.54	29.4
TOAP	−0.439	0.027	0.50	27.3

[a] Measured with respect to the standard potential for the cobaltacene/cobaltacenium couple. [b] Determined from the Tafel slope, that is, $\alpha_{ex} = -(RT/F)(d \ln k/dE)$. [c] Determined from an Arrhenius plot of standard rate constants, that is, $\Delta H^*_{ex} = -R(d \ln k_s/d(1/T))$.
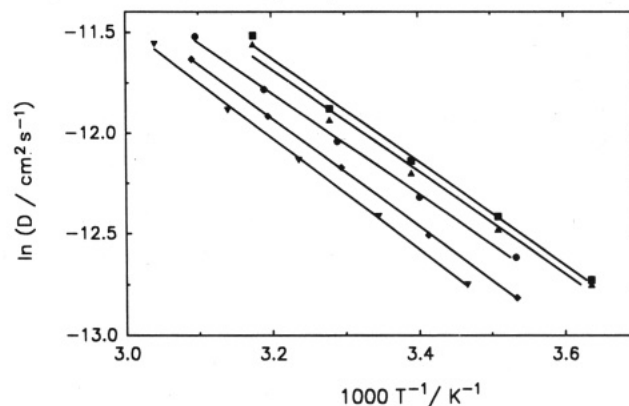

Figure 4. Logarithm of the diffusion coefficient, D, for nitromesitylene in propylene carbonate in the presence of various TAA^+ salts at 0.1 M concentration plotted against the reciprocal temperature. The TAA^+ cations are (■) TEA^+, (▲) TPA^+, (●) TBA^+, (◆) $THxA^+$, and (▼) TOA^+.

than that for larger cations. This may mean that at the potential where the present calculations have been made, the inner layer contains a significant mole fraction of solvent molecules when smaller ions such as TMA^+ and TEA^+ define the position of the outer Helmholtz plane.

Standard Potentials. In all systems investigated, plots of electrode potential against $\ln [(i_d - i)/i]$, where i is the current and i_d the diffusion limited current value in the dc voltammetric wave, were linear with a slope corresponding to a one-electron reduction process. The halfwave potentials determined from the intercept were assumed to be equal to the standard potential, E_s. Values determined in the different TAAP electrolytes are summarized in Table II. It is readily apparent that E_s is relatively independent of the nature of the TAA^+ electrolyte in agreement with observations made earlier.[4] This result suggests that ion pairing between the product anion radical NM^- and the TAA^+ cations is negligible. Some small degree of ion pairing between TEA^+ and NM^- has been suggested to occur in AN and DMF[24] and between TBA^+ and NM^- in DMF.[25] However, since PC has a much larger dielectric constant than either of these solvents, ion pairing is expected to be correspondingly weaker.

Diffusion Coefficients. Precise determination of the diffusion coefficient, D, is important in the analysis of kinetic data using the ac admittance technique.[16] Results obtained from the dc limiting current in the presence of various TAA^+ cations are shown as a function of reciprocal temperature in Figure 4. At a given temperature, the value of D decreases by about 35% when the nature of the electrolyte cation is changed from TEA^+ to TOA^+. This is attributed to a corresponding increase in solution viscosity. The viscosities of PC solutions have been studied for a wide variety of electrolytes[26] including TAA^+ salts with cations ranging from TMA^+ to $THpA^+$. These studies have been carried out both as functions of electrolyte concentration and temperature. The expected increase in viscosity with TAA^+ ion size is seen not only
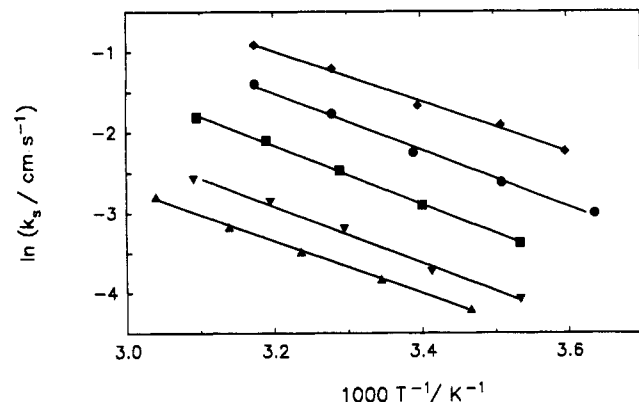
Figure 5. Logarithm of the standard rate constant for electroreduction of nitromesitylene at mercury in propylene carbonate in the presence of various TAA$^+$ salts at 0.1 M concentration plotted against the reciprocal temperature. The TAA$^+$ cations are ($\blacklozenge$) TEA$^+$, ($\bullet$) TPA$^+$, ($\blacksquare$) TBA$^+$, ($\blacktriangledown$) THxA$^+$, and ($\blacktriangle$) TOA$^+$.

in PC but also in other polar aprotic solvents.[26] It is also interesting to note that the slopes of the ln D against $1/T$ plots are constant within the experimental error, independent of the nature of the cation. This result is significant in the interpretation of the dependence of the kinetic data on cation nature as discussed below.

Kinetic Parameters. The kinetic parameters for the electro-reduction of nitromesitylene

$$NM + e^- \rightarrow NM^- \qquad (2)$$

obtained in the present study are summarized in Table II. First of all, the standard potential is constant within the experimental error indicating that change in the TAA$^+$ cations have a negligible effect on the activities of the components of the electrode reaction. On the other hand, the standard rate constant decreases by an order of magnitude when the electrolyte cation is changed from TEA$^+$ to TOA$^+$. The other two parameters, namely, the transfer coefficient, α_{ex}, and the activation enthalpy, ΔH^*_{ex}, are constant within experimental error. In the latter case, the average value is 28.2 ± 1.3 kJ mol^{-1}, the standard deviation being very close to the estimated precision for this quantity. Just as the activation enthalpy for diffusion is independent of the electrolyte so is that for electron transfer (see Figure 5). This strongly suggests that electron transfer is occuring in a medium where the properties of the solvent predominate in so far as they determine the activation parameters for the reaction.

Several reasons can be offered for the strong dependence of k_s on electrolyte composition. One explanation is that they are due to electrostatic double layer effects. However, this seems rather unlikely because the estimated electrode charge density is nearly independent of cation nature in the potential region of interest. Furthermore, double layer effects for the reaction in question are minimal, involving only a repulsive effect on the product anion radical. A second explanation is that there is a significant change in the dielectric properties of the interface with cation nature and that this change leads to either a change in the location of the reaction site, or of the dielectric properties in the vicinity of the reaction site, or a combination of both. Modern electron transfer theory predicts that the reaction medium has an effect on both the exponential and preexponential parts of the rate constant.[27-31] We will now examine the consequences of these theories with respect to both parts of the kinetic data.

The activation enthalpy for electron transfer is made up of three contributions, namely, the inner sphere reorganization enthalpy ΔH^*_{is}, the outer sphere contribution ΔH^*_{ox}, and a contribution from the temperature dependence of the solvent's longitudinal relaxation time, ΔH_L. Thus, one may write[15,32]

$$\Delta H^*_{ex} = \Delta H^*_{is} + \Delta H^*_{ox} + \theta \Delta H_L \qquad (3)$$

where θ is a fraction which depends on the degree of reaction adiabaticity and the relative magnitudes of the inner and outer sphere reorganization energies. The major contribution is assumed

to come from outer sphere reorganization in the present case, and it can be estimated according to the Born continuum model as originally described by Marcus[33] or according to the mean spherical approximation (MSA) as discussed recently by Fawcett and Blum.[34] According to the continuum treatment, ΔH^*_{ox} is given by

$$\Delta H^*_{os} = \frac{N_0 e_0^2}{32 \pi \epsilon_0 r_A} \left(\frac{1}{\epsilon_{op}} - \frac{T}{\epsilon_{op}^2} \frac{\partial \epsilon_{op}}{\partial T} - \frac{1}{\epsilon_s} + \frac{T}{\epsilon_s^2} \frac{\partial \epsilon_s}{\partial T} \right) \qquad (4)$$

where N_0 is Avogadro's constant, e_0, the electronic charge, r_A, the effective radius of the reactant, ϵ_{op}, the dielectric constant of the solvent at optical frequencies, ϵ_s, its static value, and $\partial \epsilon_{op}/\partial T$ and $\partial \epsilon_s/\partial T$, the corresponding temperature derivatives of these quantities. The effective radius for a species in which the charge density is distributed over several atoms is estimated from a model in which the reactant is represented as a collection of spheres;[35] for the case of two contiguous spheres, and neglecting the volume effect, it is given by the relationship

$$r_A = \left[\frac{f_1}{r_1} + \frac{f_2}{r_2} + \frac{2 f_1 f_2}{(r_1 + r_2)} \right]^{-1} \qquad (5)$$

where f_1 is the fraction of charge on one sphere whose radius is r_1 and f_2, the fraction on the second with radius r_2. On the basis of ESR data,[36] the estimated fraction of the charge density on the NO$_2$ group in the anion radical is 0.61. Then, assuming that the effective radius of the NO$_2$ group is 0.275 nm and that of the phenyl ring, 0.350 nm,[37] the effective radius for the nitromesitylene system is 0.392 nm. Using tabulated data for the dielectric constants and their temperature coefficients,[19,38] the estimate of ΔH^*_{os} for the NM/NM$^-$ system in PC at 25 °C is 18.6 kJ mol^{-1}, a result which is significantly less than the experimental value (28.2 kJ mol^{-1}). The experimental value of ΔH^* for the same reaction in DMF is 17.6 kJ mol^{-1}, and the estimate for ΔH^*_{os} on the basis of eq 4, 18.1 kJ mol^{-1}. These results indicate that the major difference between the experimental activation enthalpies in the two solvents is due to the temperature dependence of solvent relaxation. Nevertheless, the Born continuum estimates of ΔH^*_{ox} are clearly too high and indicate a negligible contribution from ΔH_L in DMF. On the basis of the MSA,[34] the expression for ΔH^*_{os} is

$$\Delta H^*_{os} = \frac{N_0 e_0^2}{32 \pi \epsilon_0} \left[\left(1 - \frac{1}{\epsilon_s} - \frac{T}{\epsilon_s^2} \frac{\partial \delta_s}{\partial T} \right) \frac{1}{(r_A + \delta_s)} + \left(1 - \frac{1}{\epsilon_s} \right) \frac{T}{(r_A + \delta_s)^2} \frac{\partial \delta_s}{\partial T} - \left(1 - \frac{1}{\epsilon_{op}} - \frac{T}{\epsilon_{op}^2} \frac{\partial \epsilon_{op}}{\partial T} \right) \frac{1}{r_A} \right] \qquad (6)$$

where δ_s is the ratio of the radius of the solvent represented as a sphere, r_s, to the MSA polarization parameter, λ, and $\partial \delta_s/\partial T$, its temperature coefficient. Values of δ_s and $\partial \delta_s/\partial T$ appropriate for reactions involving anions in the solvents discussed here have been tabulated recently[32] on the basis of thermodynamic data for monovalent monoatomic anions, namely, the halides. Using these parameters, the MSA estimates of ΔH^*_{os} for spherical reactants with a radius of 0.392 nm are 16.4 kJ mol^{-1} in PC and 16.6 kJ mol^{-1} in DMF. Although it may not be correct to use values of δ_s appropriate for spherical reactants with the present system, the estimates are only slightly smaller than the Born estimates as is generally the case for anionic systems.[15,32,34] Thus, on the basis of current theory, the large difference in ΔH^*_{ex} between the PC and DMF systems is probably due to dynamical solvent effects.

In order to assess the contribution from the dynamical solvent effect, one must have an estimate of the coefficient θ. This may be found[39] on the basis of a plot of the logarithm of the standard rate constant at constant temperature in different solvents against the logarithm of the longitudinal relaxation time τ_L. A plot of data obtained earlier[4,10] in five aprotic solvents with 0.1 M TEAP as electrolyte is shown in Figure 6. From the slope of this plot the value of θ is 0.5. Using the values of ΔH_L estimated earlier[32]
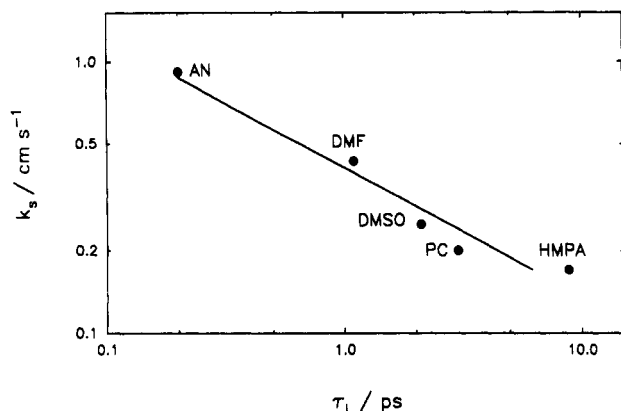
Figure 6. Plot of the standard rate constant for electroreduction of nitromesitylene at mercury in five different solvents with 0.1 M TEAP as electrolyte against the solvent's longitudinal relaxation time using logarithmic scales on both axes. The solvents are indicated with DMSO corresponding to dimethyl sulfoxide and HMPA, to hexamethylphosphoramide.

Figure 7. Plot of the logarithm of the standard rate constant for electroreduction of nitromesitylene (NM) and 2-nitropropane (NP) at mercury in the presence of various TAA^+ cations against the cation's crystallographic radius r_+ corrected by a constant amount δ. In the case of the data designated (●) the correction is zero, and in the case of the data designated (▲), the correction is 0.37 nm for cations with $n > 3$, or r_+ for cations with $n \leq 3$ (eq 7).

and assuming that ΔH^*_{is} is zero, the estimates of ΔH^*_{ex} are 23.1 kJ mol^{-1} in PC and 20.0 kJ mol^{-1} in DMF. On the basis of the discussion by Allendoefer and Rieger,[36] is is probable that some internal reorganizational work is involved in forming the anion radical of NM. Addition of 5 kJ mol^{-1} would bring the estimate ΔH^*_{ex} in PC in agreement with the experimentally observed value, but the estimate in DMF would then be 7 kJ mol^{-1} higher than the experimental value. Considering the level of error normally expected in determining the activation enthalpy (± 2 kJ mol^{-1}), the agreement between theory and experiment is acceptable. In order to access these results more carefully, a theoretical estimate of ΔH^*_{is} is necessary.

The above calculations have been made assuming that the reaction takes place in a medium with approximately the same dielectric properties as those of the solvent. Indeed, the present results and those obtained earlier by Petersen and Evans[6] give strong support to this conclusion. If the reaction took place in a medium with dielectric properties of the tetraalkylammonium ions, one would expect the local dielectric constant to be much lower. In this case, the Gibbs energy and enthalpy of activation would be at least an order of magnitude smaller. This follows from the fact that the optical dielectric constant for solvents such as hexane, whose properties are expected to be close to those of tetraalkylammonium ions under the electrostrictive pressure of the electrode field, is only slightly smaller than the static dielectric constant. Thus, the Pekar factor, $(1/\epsilon_{op} - 1/\epsilon_s)$, in these media is very small compared to the value found for most polar solvents (~ 0.5). On the basis of the present results, it is concluded that electroreduction of NM involves electron tunneling through a layer of tetraalkylammonium cations adsorbed on the electrode in agreement with the earlier conclusion by Petersen and Evans.[6]

According to the theory of electron tunneling from a film covered electrode to a redox species in solution,[40-42] the dependence of the standard rate constant on film thickness is given by

$$k_s = k_{so}e^{-\beta d_f} \qquad (7)$$

where k_{so} is the standard rate constant for the uncovered electrode, d_f, the thickness of the film for electron tunneling, and β, a parameter which depends on the barrier height for electron tunneling. This theory has been examined with respect to electron tunneling through adsorbed monolayers on electrodes[42-44] and was used by Evans and Gilicinski[7] to analyze the effects of TAA^+ ions on heterogeneous electron transfer to nitroalkanes and diketones. A plot of the values of ln k_s observed in various TAA^+ solutions against the crystallographic radius of the TAA^+ cation is shown in Figure 7. Also included in this plot are the data reported by Evans and Gilicinski[7] for the electroreduction of 2-nitropropane (NP) in AN. Excellent linear correlations are obtained in both cases, the slope of the plot being greater for the NP system. The parameter, β, cannot be obtained directly from these plots because
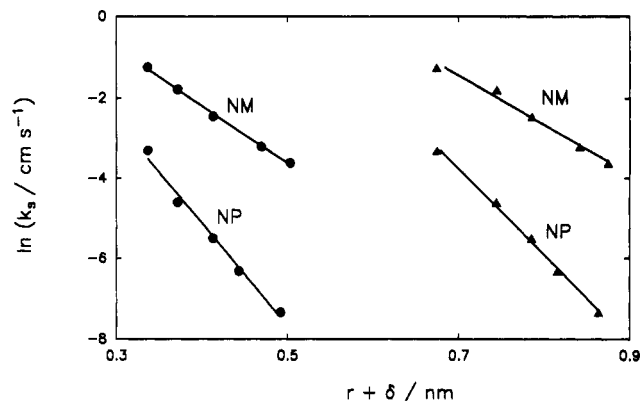
there is no direct relationship between the electron tunneling distance, d_f, and the crystallographic radius, r_+. However, on the basis of the results presented here for two systems which have been studied at different potentials and in different solvents, the relationship is undoubtedly quite simple. If one assumes that $d_f = 2r_+$ as was done earlier,[7] then β is equal to 7.2 nm^{-1} for the NM system and 13 nm^{-1} for the NP system. On the basis of the analysis of the capacity data, this estimate of d_f is too large because it does not consider the probable bending of the alkyl arms of the TAA^+ ion in the electrode field (Figure 3). On the basis of the analysis of the capacity data a more reasonable relationship between d_f and r_+ is

$$d_f = 2r_+, \qquad n \leq 3 \qquad (7a)$$

or

$$d_f = r_+ + 0.37, \qquad n > 3 \qquad (7b)$$

Thus, it is assumed that the three of the tetrahedrally disposed alkyl groups in the TAA^+ ion are pointed toward the surface, and, in the case of the larger ions, are bent so that the charge center at the nitrogen atom approaches a distance of 0.37 nm to the surface in the case of the larger ions. One alkyl group is assumed to point out into the solution, and the space between adjacent adsorbed TAA^+ ions to be filled with alkyl groups from ions which have their charge centers further away from the interface. As can be seen from Figure 7, equally good correlations between ln k_s and d_f are obtained when the tunneling distance is estimated on the basis of eq 7. The estimates of β are then 12 nm^{-1} for the NM system and 22 nm^{-1} for NP, results which are similar to those obtained in other studies.[7,42-44] The higher barrier height for the NP system is attributed to the fact that this process occurs at a significantly more negative potential, but the solvent undoubtedly plays a role as well.

It should be mentioned that one would expect a change in the longitudinal relaxation time for the solvent PC with change in electrolyte composition. However, this change is quite small[12] and certainly not enough to explain the observed change in rate constant with size of the TAA^+. Our conclusion is supported by theoretical considerations regarding the effect of electrolyte on solvent relaxation processes.[45]

It should also be pointed out that the relationship used here to estimate ΔH^*_{os} assumes that the effect of images formed in the electrode or in the layer of low dielectric constant composed of TAA^+ ions is negligible. This assumption, which was tested previously on the basis of a comparison of results for homogeneous and heterogeneous electron transfer,[46] is supported by the present results. Development of a model for imaging considering three regions, namely, the metal, a low dielectric constant adsorbed organic layer, and finally, a high dielectric constant electrolyte

solution would be helpful in considering this question further.

In conclusion, it seems clear from the present study that TAA$^+$ ions form a blocking layer at negative potentials on a polarizable electrode when they are adsorbed from aprotic solvents. The thickness of this layer increases with the length of the alkyl chain but is not simply related to the crystallographic radius of the TAA$^+$ ion as is seen from differential capacity data. Electron transfer occurs by tunneling through the resulting organic layer, more probably by elastic transitions,[42] to the redox system in solution. Much more needs to be learned about this process, and further experiments should be carried out. These should involve a series of structurally similar redox systems of relatively simple nature but with a wide range of standard potentials. The role of the solvent also needs to be further elucidated as far as the tunneling process is concerned.

References and Notes

(1) Baranski, A. S.; Fawcett, W. R. *J. Electroanal. Chem.* **1979,** *100,* 287.
(2) Corrigan, D. A.; Evans, D. C. *J. Electroanal. Chem.* **1980,** *106,* 287.
(3) Rüssel, C.; Jaenicke, W. *J. Electroanal. Chem.* **1984,** *180,* 205.
(4) Kapturkiewicz, A.; Opallo, M. *J. Electroanal. Chem.* **1985,** *185,* 15.
(5) Gennett, T.; Weaver, M. J. *J. Electroanal. Chem.* **1985,** *186,* 179.
(6) Petersen, R. A.; Evans, D. H. *J. Electroanal. Chem.* **1987,** *222,* 129.
(7) Evans, D. H.; Gilicinski, A. G. *J. Phys. Chem.* **1992,** *96,* 2528.
(8) Fawcett, W. R. *Can. J. Chem.* **1981,** *59,* 1844.
(9) Peover, M. E.; Powell, J. E. *J. Electroanal. Chem.* **1969,** *20,* 427.
(10) Fawcett, W. R.; Lasia, A. *J. Phys. Chem.* **1978,** *82,* 1114.
(11) Saveant, J. M.; Tessier, D. *J. Chem. Soc., Faraday Dis.* **1982,** *74,* 57.
(12) Barthel, J.; Feuerlein, F. *J. Solution Chem.* **1984,** *13,* 393.

(13) Kuznetsov, V. A.; Vasil'kevich, N. G.; Damaskin, B. B. *Elektrokhimiya* **1970,** *6,* 1339.
(14) Fawcett, W. R.; Foss, C. A., Jr. *J. Electroanal. Chem.* **1988,** *250,* 225.
(15) Fawcett, W. R.; Opallo, M. *J. Electroanal. Chem.* **1992,** *331,* 815.
(16) Yee, S. Ph.D. Dissertation, University of California, Davis, 1991.
(17) Fawcett, W. R.; Yee, S. *J. Electroanal. Chem.* **1988,** *248,* 327.
(18) Andreu, R.; Sluyters-Rehbach, M.; Remijnse, A. G.; Sluyters, J. H. *J. Electroanal. Chem.* **1982,** *134,* 101.
(19) Marcus, Y. *Ion Solvation;* Wiley-Interscience: New York, 1985.
(20) Gambert, R.; Baumgartel, H. *J. Electroanal. Chem.* **1985,** *183,* 315.
(21) Fawcett, W. R.; Loutfy, R. O. *Can. J. Chem.* **1973,** *51,* 230.
(22) Fawcett, W. R.; Ikeda, B. M.; Sellan, J. B. *Can. J. Chem.* **1979,** *57,* 2268.
(23) Nielaba, P.; Knowles, T.; Forstmann, F. *J. Electroanal. Chem.* **1985,** *183,* 329.
(24) Chauhan, B. G.; Fawcett, W. R.; Lasia, A. *J. Phys. Chem.* **1977,** *81,* 1476.
(25) Jaworski, J. S. *J. Electroanal. Chem.* **1987,** *219,* 209.
(26) Karapetyan, Yu. A.; Ejchis, V. N. *Physicochemical Properties of Non-Aqueous Electrolyte Solutions* (in Russian); Chimia: Moscow, 1989, Chapter 2.
(27) Zusman, L. D. *Chem. Phys.* **1980,** *51,* 449.
(28) Ovchinnikova, M. Ya. *Theo. Exp. Khim.* **1981,** *17,* 651.
(29) Van der Zwan, G.; Hynes, J. T. *J. Chem. Phys.* **1982,** *76,* 2293.
(30) Calef, D. F.; Wolynes, P. G. *J. Phys. Chem.* **1983,** *87,* 3387.
(31) Sumi, H.; Marcus, R. A. *J. Electroanal. Chem.* **1986,** *204,* 59.
(32) Fawcett, W. R.; Opallo, M. *J. Phys. Chem.* **1992,** *96,* 2920.
(33) Marcus, R. A. *J. Chem. Phys.* **1965,** *43,* 679.
(34) Fawcett, W. R.; Blum, L. *Chem. Phys. Lett.* **1991,** *187,* 173.
(35) Fawcett, W. R.; Kharkats, Yu. I. *J. Electroanal. Chem.* **1973,** *47,* 413.
(36) Allendoefer, R. D.; Rieger, P. H. *J. Am. Chem. Soc.* **1966,** *88,* 3711.
(37) Peover, M. E.; Powell, J. S. *J. Electroanal. Chem.* **1969,** *20,* 427.
(38) Riddick, J. A.; Bunger, W. B. *Organic Solvents;* Wiley-Interscience: New York, 1970.
(39) Fawcett, W. R.; Foss, C. A., Jr. *Electrochim. Acta* **1991,** *36,* 1767.
(40) Schultze, J. W.; Vetter, K. J. *Electrochim. Acta* **1973,** *18,* 889.
(41) Schmickler, W. *J. Electroanal. Chem.* **1977,** *82,* 65.
(42) Lipkowski, J.; Buess-Hermann, C.; Lambert, J. P.; Gierst, L. *J. Electroanal. Chem.* **1986,** *202,* 169.
(43) Miller, C.; Cuendet, P.; Grätzel, M. *J. Phys. Chem.* **1991,** *95,* 877.
(44) Finklea, H. O.; Hanshew, D. D. *J. Am. Chem. Soc.* **1992,** *114,* 3173.
(45) Chapman, C. F.; Maroncelli, M. *J. Phys. Chem.* **1991,** *95,* 9095.
(46) Baranski, A. S.; Winkler, K.; Fawcett, W. R. *J. Electroanal. Chem.* **1991,** *313,* 367.

Formation of Ordered Structures in the Thin-Film Amorphous Carbon/Silicate Glass System

K. Starbova,* **D. Kozhuharova, N. Starbov,**

Central Laboratory of Photographic Processes, Bulgarian Academy of Sciences, 1113 Sofia, Bulgaria

and V. Tonchev

Institute of Physical Chemistry, Bulgarian Academy of Sciences, 1113 Sofia, Bulgaria
(Received: June 22, 1992)

A system thin film of amorphous carbon arc evaporated in vacuum on glass substrate is studied. By applying suitable decoration procedures, microscopic defects having spirallike symmetry are visualized in the glass substrate. It is established that the value of the background pressure in the vacuum chamber, the film thickness, and the chemical composition of the substrate surface are basic factors determining the spiral formation. The peculiarities in the spiral morphology give the reason the observed structures to be regarded as a result of a self-organization phenomenon.

Introduction

The interest toward ordered structures formed as a result of self-organization phenomena in various physical, chemical, and biological systems has considerably increased following the discovery of organizing centers in the Belousov–Zhabotinski (BZ) reaction.[1] Depending on the experimental conditions, different types of autowave structures can be initiated such as "target" patterns, "fronts", and spiral waves resulting from "front" breaking,[2] spirals with a topological charge greater than unity,[3,4] and the quasi-stochastic regime.[5,6] In fact such structures have already been observed but they have been regarded as Liesegang rings.[7-11] Recently, a complete set of these self-organization phenomena has been obtained during electrodeposition of Ag–Sb metal alloys.[12]

* To whom correspondence should be addressed.